Final Report

Physics of Complex Networks: Structure and Dynamics

Università degli Studi di Padova

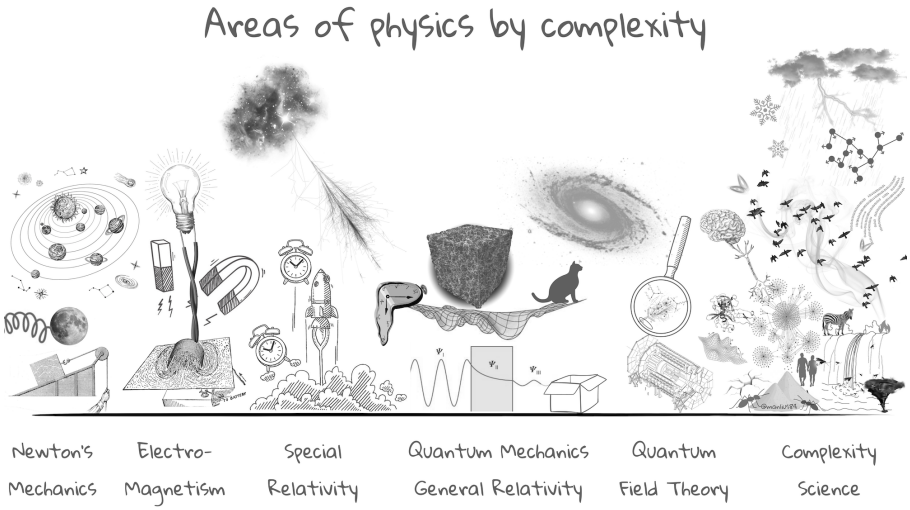

Project # 7: Epidemic spreading on networks: SI, SIS, SIR, SEIR in homogeneous and heterogeneous approximation

Bedin Veronica

Last update: July 12, 2025

Contents

1 | Static networks, homogeneous mean field approximation

Task leader(s): *Veronica Bedin*

1.1 | Epidemics modeling

Epidemic modeling began with Kermack and McKendrick's 1927 work [1] and became a key tool in epidemiology. Its role was pivotal during COVID-19 for tracking transmission and guiding interventions [2, 3, 4]. Compartmental models are the most widely used approach, aiming to describe population-level dynamics from individual contagion processes. Each individual is in state n at time t.
Depending on the model we are considering, the states are different:

1. **S**: susceptible, the individual is healthy but susceptible to the disease
2. **E**: exposed, the individual has been exposed to the disease.
3. **I**: infected, the individual is ill and capable of infection.
4. **R**: recovered, the individual recovered from the illness (or died) and is no longer infectable.

The most widely used compartmental models are the following:

1. ***SI***: The *SI* model is applicable to diseases in which recovery does not occur. The population is divided into susceptible S and infected I. The infection process is modeled by the reaction:
$$S + I \xrightarrow{\beta} I + I$$
β is the probability per unit of time that an individual S becomes I upon contact with an individual I.
2. ***SIS***: The *SIS* model applies to infections that do not confer lasting immunity. In this case, individuals return to the susceptible compartment after recovery:
$$S + I \xrightarrow{\beta} I + I$$
$$I \xrightarrow{\mu_S} S$$
μ_S, is the rate at which an individual becomes S again, the inverse of infection time τ_I.

3. ***SIR***: The *SIR* model applies to infections that confer lasting immunity (or death). In this case, individuals move to the recovered compartment after recovery:

$$S + I \xrightarrow{\beta} I + I$$
$$I \xrightarrow{\mu_R} R$$

μ_R, the rate at which an individual recovers, the inverse of infection time τ_I, where τ_I is the duration of infection.

4. ***SEIR***: The *SEIR* model incorporates a latent period between exposure and infectiousness: individuals do not become infectious immediately after being infected.

$$S + I \xrightarrow{\beta} I + E$$
$$E \xrightarrow{\alpha} I$$
$$I \xrightarrow{\mu} R$$

β_E is the *exposion rate*. α is the rate at which an individual becomes infected, the inverse of exposion time τ_E.

Some quantities of interest in epidemic modeling include:

- The *basic reproduction number* R_0 average number of secondary infections produced by a single infected individual in a fully susceptible population.
- *Effective reproduction number* $R(t)$: secondary cases per case at time t.
- *Critical epidemic threshold*: the critical value of parameter β above which an epidemic can invade the network.

1.2 | Homogeneous Mean-Field Approximation

The objective of this review is to simulate the behavior of well-known epidemic models and analyze their dynamics, particularly focusing on critical phenomena such as the epidemic threshold. To do so, I compare computational simulations run on networks with analytical predictions derived under the *homogeneous mean-field* (HMF) approximation. This approximation assumes a network with bounded or uniform degree, i.e., $k_i \simeq \langle k \rangle$, allowing each node to be treated statistically equivalently.

A deeper treatment of the models and governing ODEs is provided in Appendix 4.2, where *SI*, *SIR*, and *SEIR* are described. Here, I focus on the *SIS* model, both analytically and via simulation.

1.2.1 *SIS* Dynamics on Homogeneous Networks

To formulate the *SIS* model on a general network, we define a binary state variable $\sigma_i(t)$, which is 1 if node i is infected and 0 if susceptible. Let $\rho(i,t) = \text{Prob}[\sigma_i(t) = 1]$. The evolution equation is:

$$\frac{d\rho(i,t)}{dt} = -\mu\rho(i,t) + \beta \sum_j A_{ij} \text{Prob}[\sigma_i(t) = 0, \sigma_j(t) = 1] \tag{1.1}$$

This form is not closed due to correlations between neighbors. Under the HMF approximation and assuming spatial homogeneity $\rho(i,t) = \rho(t)$, we factor the joint probability: $\text{Prob}[\sigma_i = 0, \sigma_j = 1] \approx (1-\rho)\rho$. Equation (1.1) becomes:

$$\frac{d\rho}{dt} = -\mu\rho + \beta\langle k\rangle(1-\rho)\rho \tag{1.2}$$

Throughout this work, in all specific model analyses, we set $\mu_S = \mu$ or $\mu_R = \mu$ to simplify the notation without loss of generality.

For a detailed derivation of these calculations, see Appendix 4.2.2.

This mean-field ODE predicts an epidemic threshold at $\beta_c = \mu/\langle k\rangle$. For $\beta > \beta_c$, an endemic equilibrium $\rho^* > 0$ is reached.

1.2.2 Comparison with Simulations

I simulate the *SIS* model on an Erdős-Rényi network with $N = 10000$ and average degree $\langle k\rangle \approx 8$. The simulation implements the stochastic infection and recovery process node by node. Further information about the simulation process can be found in Section 4.1. Snapshots and density evolution are shown below.

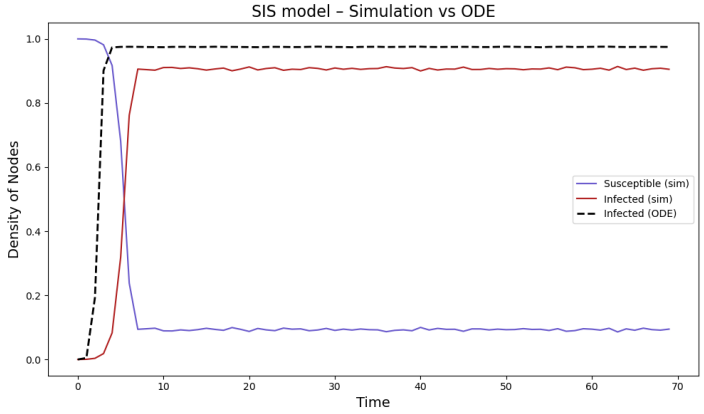

Figure 1.1: Time evolution of the density of susceptible (blue) and infected (red) individuals. In black the analytical Homogeneous MF evolution of the infected.

The simulation results exhibit a non-zero steady-state infected density, qualitatively consistent with the ODE prediction in Equation (4.6). However, noticeable differences between the analytical and simulated curves appear even at early times. These deviations are primarily due to finite-size effects and stochastic fluctuations which are not captured by the mean-field approximation.

Here, I focused on the *SIS* model. The remaining models (*SI*, *SIR*, *SEIR*), along with their governing equations and analytical solutions, are provided in Section 4.2.

1.2.3 Threshold Estimation

I also numerically estimate the critical threshold β_c by running the simulation for increasing β (10 times for each β) and observing whether the infection dies out or

reaches an endemic state. Figure 1.2 illustrates the epidemic threshold for the *SIS* model by comparing the simulated infected density with the analytical prediction. The theoretical threshold is $\beta_c = 0.005$, very close to the one obtained in the simulations.

I do not include similar threshold plots for the other models: in the *SI* model, the concept of a threshold is not meaningful because infection spreads irreversibly without recovery, while the *SIR* and *SEIR* models display a threshold behavior qualitatively similar to the *SIS* case.

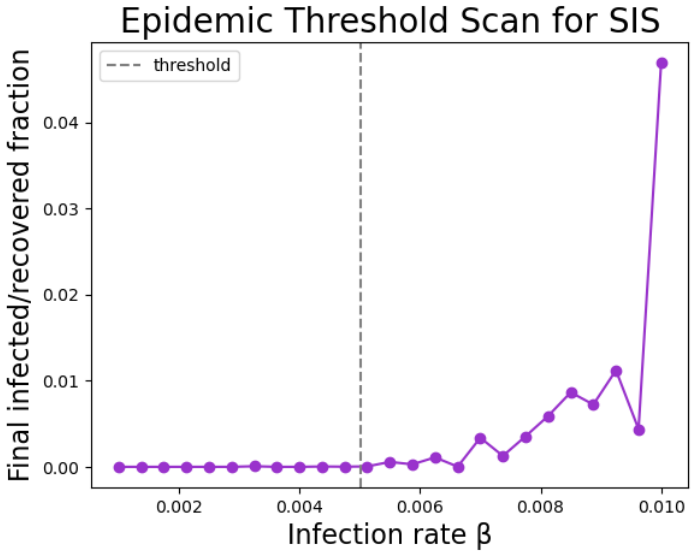

Figure 1.2: Steady-state of infected density as a function of β. The gray line is the theoretical threshold

In simulations, the observed threshold is compatible with the one we obtain through theory. At $\beta_c = 0.005$ we observe the first onset of the disease.

2 | Static networks, heterogeneous mean field approximation

Task leader(s): *Veronica Bedin*

2.1 | Heterogeneous Mean-Field Approximation

To capture the dynamics of epidemics on networks with broad degree distributions, such as scale-free networks, a more refined analytical approach is needed. In these systems, high-degree nodes (hubs) play a disproportionate role in transmission, making the homogeneous mean-field approximation insufficient. Instead, I adopt the *heterogeneous mean-field* (HMF) approximation, which accounts for degree-dependent infection probabilities. This approach is called *Degree based mean field approach*

This framework is particularly relevant for networks where the degree distribution follows a power law, as discussed in the seminal work by Pastor-Satorras and Vespignani [5]. In what follows, I focus again on the *SIS* model to explore the implications of network heterogeneity on the epidemic threshold and spreading dynamics.

A deeper treatment of the models and governing ODEs is provided in Appendix 4.3, where *SI*, *SIR*, and *SEIR* are described. Here, I focus analytically on the *SIS* model.

2.1.1 *SIS* Dynamics on Heterogeneous Networks

To formulate the *SIS* model within the heterogeneous mean-field approximation, we divide nodes into compartments based on their degree. Let

$$s_k = \frac{S_k}{N_k}, \qquad \rho_k = \frac{I_k}{N_k},$$

where s_k and ρ_k denote the fractions of susceptible and infected nodes of degree k, and N_k is the total number of nodes with degree k.

This leads to a system of differential equations, one for each degree class:

$$\frac{d\rho_k(t)}{dt} = -\mu\rho_k(t) + \beta k \left(1 - \rho_k(t)\right) \Theta_k(t), \tag{2.1}$$

where $\Theta_k(t)$ is the probability that a neighbor of a node with degree k is infected. It is given by:

$$\Theta_k(t) = \sum_{k'} P(k'|k)\rho_{k'}(t).$$

Assuming no degree correlations, the conditional probability becomes:

$$P(k'|k) = \frac{k'P(k')}{\sum_{k'} k'P(k')} = \frac{k'P(k')}{\langle k \rangle},$$

and thus:

$$\Theta_k(t) = \frac{\sum_{k'} k'P(k')\rho_{k'}(t)}{\langle k \rangle} = \Theta(t),$$

which shows that $\Theta(t)$ becomes independent of k.

At steady state, where $\frac{d\rho_k(t)}{dt} = 0$, we find:

$$\rho_k = \frac{\beta k \Theta}{\mu + \beta k \Theta}.$$

Substituting this expression into the definition of Θ yields a self-consistent equation:

$$\Theta = \frac{1}{\langle k \rangle} \sum_k \frac{k^2 P(k) \beta \Theta}{\mu + \beta k \Theta} = f(\Theta).$$

To determine whether a non-trivial solution ($0 < \Theta \leq 1$) exists, we analyze the derivative at $\Theta = 0$:

$$\frac{d}{d\Theta} \left(\frac{1}{\langle k \rangle} \sum_k \frac{k^2 P(k) \beta \Theta}{\mu + \beta k \Theta} \right) \Bigg|_{\Theta=0} \geq 1,$$

which leads to the condition:

$$\frac{\beta}{\mu \langle k \rangle} \sum_k k^2 P(k) \geq 1,$$

or equivalently,

$$\frac{\beta \langle k^2 \rangle}{\mu \langle k \rangle} \geq 1.$$

This inequality determines the onset of an *endemic state*. The corresponding epidemic threshold is:

$$\beta_c = \frac{\mu \langle k \rangle}{\langle k^2 \rangle}.$$

For homogeneous networks, where $\langle k^2 \rangle = \langle k \rangle^2$, we recover the standard threshold. However, in scale-free networks with $2 < \gamma < 3$, the moments behave as $\langle k \rangle \to c$ and $\langle k^2 \rangle \to \infty$ as $N \to \infty$. In this limit: $\beta_c \to 0$ implying that the epidemic threshold vanishes in the thermodynamic limit. As a result, any disease, no matter how weakly infectious, can propagate through the network. Thresholds are explored in the Section 4.3.5.

I will perform the same analysis for the *SIR* model in the Supplementary Material (see Appendix 4.3), where I also derive the expected finite-size effects for *SIS*. In particular, I expect to observe:

$$\beta_c \simeq \left(\frac{\mu k_c}{k_m in} \right)^{\gamma - 3}$$

3 | Patchy metapopulations, homogeneous mean field approximation

Task leader(s): *Veronica Bedin*

3.1 | Metapopulation diffusion models

Metapopulation models provide a powerful framework for studying epidemic dynamics in spatially structured populations, where individuals reside in discrete subpopulations (or patches) and interact both locally and via migration [6, 7]. Each patch hosts standard compartmental dynamics (e.g., SI, SIR), while individuals move across a mobility network, coupling the local epidemics. This approach allows for the identification of both local epidemic thresholds and global invasion thresholds, which depend on the interplay between disease parameters and network topology [8]. These models have been fundamental in understanding real-world epidemic spread and mobility effects.
A reaction–diffusion framework, commonly used in physical and chemical systems, can be adapted to model epidemic dynamics on networks. In this context, each subpopulation (or patch) i is characterized by an occupation number N_i, representing the number of individuals in that patch, with the total population of the model given by $N = \sum_i N_i$. Individuals diffuse across the network along edges, with a diffusion coefficient d_{ij} that may depend on node degrees, subpopulation sizes, or an external mobility matrix.

3.2 | Derivation of the Invasion Threshold in the Homogeneous Metapopulation Case

This derivation follows the framework described in [6]. We consider a homogeneous metapopulation network in which each patch has the same degree $\bar{k}$ and population size $\bar{N}$. Local outbreaks are assumed to occur when the basic reproductive number within a patch satisfies $R_0 > 1$, so that a fraction $\alpha\bar{N}$ of individuals becomes infected during the course of the outbreak. α depends on the specific disease model used and the disease parameter values.

Each infected individual remains infectious for an average duration μ^{-1} and travels to one of its $\bar{k}$ neighbors at rate d. Therefore, the expected number of new infected seeds transmitted from patch i to neighbor j during a local outbreak is:

$$\lambda_{\bar{k}\bar{k}} = d\frac{\alpha\bar{N}}{\mu}.$$

Using a tree-like approximation—which assumes that the metapopulation connectivity graph has no loops at the scale of the spreading process, i.e., during the early stages of the epidemic, it is unlikely that an infected patch is reinfected via another path—we let D_n be the number of infected patches in generation n. This approximation allows us to model the early spread as a branching process. Each infected patch in generation $n-1$ spreads seeds to its $\bar{k}-1$ neighbors (excluding the parent patch).

$$D_n = D_{n-1}(\bar{k}-1)\left[1-\left(\frac{1}{R_0}\right)^{\lambda_{\bar{k}\bar{k}}}\right]\left(1-\frac{D^{n-1}}{V}\right)$$

with V number of nodes.
The simplest case of homogeneous diffusion of individuals $d_{\bar{k}} = p/\bar{k}$ yields to $\lambda_{\bar{k}\bar{k}} = p\bar{N}\alpha\mu^{-1}/\bar{k}$.

Assuming that each seed causes a successful local outbreak with probability $\approx R_0 - 1$ (valid for $R_0 - 1 \ll 1$), we obtain:

$$\left[1-\left(\frac{1}{R_0}\right)^{\lambda_{\bar{k}\bar{k}}}\right] \simeq \lambda_{\bar{k}\bar{k}}(R_0-1) \tag{3.1}$$

Assuming also that we are in the early stages, hence $D^{n-1}/V \ll 1$, we obtain

$$D_n = p\bar{N}\alpha\mu^{-1}\frac{\bar{k}-1}{\bar{k}}(R_0-1)D_{n-1}. \tag{3.2}$$

Thus, the number of infected patches grows when:

$$p\bar{N}\alpha\mu^{-1}\frac{\bar{k}-1}{\bar{k}}(R_0-1) > 1.$$

Defining the *global invasion threshold* R^* as:

$$R^* = p\bar{N}\alpha\mu^{-1}\frac{\bar{k}-1}{\bar{k}}(R_0-1) \tag{3.3}$$

we require $R^* > 1$ for global invasion.

Form Equation 3.3 is possible to write the threshold condition on the mobility rate d:

$$d^{-1} < \frac{(\bar{k}-1)\,a\,\bar{N}\,(R_0-1)}{\mu}.$$

that fixes the threshold in the diffusion rate of individuals for the global spread of the epidemic in the metapopulation systems.

As pointed out in [9], the global spread of epidemics in structured populations is influenced not only by the basic reproductive number R_0, but also by factors such as the infectious period and the mobility process.

In the *SIR* model, for values of R_0 slightly above 1, the final size of the outbreak in a single patch, denoted by the constant α, can be approximated as [10]:

$$\alpha \approx 2\frac{\mu}{\beta}\left(1-\frac{\mu}{\beta}\right) = \frac{2(R_0-1)}{R_0^2}.$$

This approximation leads to a condition for the critical mobility rate that allows global invasion of the epidemic in a homogeneous metapopulation network:

$$p\bar{N} \geq \frac{\bar{k}}{\bar{k}-1} \cdot \frac{\mu R_0^2}{2(R_0-1)^2}, \tag{3.4}$$

This result shows that the closer R_0 is to the epidemic threshold, the higher the mobility rate must be to ensure the infection spreads across patches. For larger values of R_0, this approximation becomes invalid, and the invasion threshold must be computed using more complex, implicit expressions. Further evaluations of the *Invasion threshold* for *SI,SIS* and *SEIR* can be found in Section 4.4 —

Key implications:

- There are **two thresholds** in metapopulation models:
  1. Local threshold $R_0 > 1$, ensuring each patch can sustain an outbreak.
  2. Global threshold $R^* > 1$, ensuring the spread from patch-to-patch.
- The threshold on travel/mobility rates is inversely proportional to $(\bar{k}-1)(R_0-1)$, indicating that larger connectivity and higher local transmissibility lower the required diffusion rate for global spread.
- This framework correctly predicts the limited efficacy of travel restrictions: the mobility rate d must be reduced by orders of magnitude to halt global invasion, consistent with simulation results and historical pandemic data [6, 11].

4 | Supplementary material

Task leader(s): *Veronica Bedin*

4.1 | Numerical Simulation of Epidemic Models on Networks

In this section, I describe the computational procedure adopted to simulate the spreading dynamics of different compartmental epidemic models over a network. The evolution is governed by a discrete-time stochastic process, where each node updates its state according to probabilistic transition rules defined by the model parameters and the state of its neighbors.

At each time step, the number of nodes in each compartment is recorded to reconstruct the time evolution of the epidemic. Additionally, I store snapshots of the network state at three distinct time points (initial, intermediate, and final), to visualize the spatial progression of the disease. For each model, I also compute the critical threshold, evaluating the fraction of Recovered or Infected (depending on the model) at the end of the simulation for different values of β

The simulations are performed on synthetic graphs generated using network models such as Erdős-Rényi in the homogeneous case and Barabàsi-Albert in the heterogeneous one, where each node is initially assigned a state (typically all susceptible except for one randomly infected individual).

4.1.1 SI Model

In the SI model, each susceptible node can become infected upon contact with an infectious neighbor. The probability of infection from each infectious neighbor is governed by the infection rate β. Once infected, nodes remain infectious forever. At each time step, for every susceptible node, the number of infectious neighbors is counted. The probability that the node avoids infection from all its infected neighbors is $(1-\beta)^{k_I}$, where k_I is the number of infectious neighbors. Hence, the probability that the node becomes infected is:

$$P_{\text{infect}} = 1 - (1-\beta)^{k_I}$$

4.1.2 SIS Model

The SIS model extends the SI model by allowing infectious nodes to recover and return to the susceptible state with probability μ_S

At each time step, susceptible nodes are updated as in the SI model. Infectious nodes have a probability μ_S to become susceptible again. This model can sustain an endemic equilibrium depending on the parameters and the underlying network structure.

4.1.3 SIR Model

In the SIR model, infectious nodes recover permanently and move to the recovered state, from which they can no longer participate in the dynamics. As with SIS, transitions for S and I are governed by probabilistic rules at each time step. The epidemic dies out when no more infectious nodes remain.

4.1.4 SEIR Model

The SEIR model introduces an additional exposed state E to account for the incubation period between infection and becoming infectious. Susceptible nodes move to the exposed state with probability $1-(1-\beta)^{k_I}$. Exposed nodes become infectious with probability α, and infectious nodes recover with probability μ.

4.2 | Homogeneous Mean Field approximation

In this appendix, I analyze epidemiological models under the homogeneous mean-field approximation and compare them with network-based simulations. This method assumes that all nodes have approximately the same degree and that the population is well mixed.

This approximation replaces the sum over neighbors in the microscopic description $\sum_j A_{ij}$ with the average degree $\langle k \rangle$, removing network structure. For example, for the SIS model, the full probabilistic evolution is:

$$\frac{d\rho}{dt} = -\mu\rho + \beta \sum_j A_{ij}(1-\rho)\rho, \tag{4.1}$$

with ρ probability of being infected. This becomes

$$\frac{d\rho}{dt} = -\mu\rho + \beta\langle k \rangle(1-\rho)\rho, \tag{4.2}$$

after applying the homogeneous mean-field assumption. This justifies the use of $\beta\langle k \rangle$ in all equations below.

4.2.1 Network Setup and Simulation Parameters

The simulations are performed on an Erdős–Rényi (E–R) network with $N = 10000$ nodes and connection probability $p = 0.002$. The total simulation time is $T = 70$. The average degree is $\langle k \rangle \sim 8$

Infection rate β, Exposion rate β_E	0.2
Rate S μ_S, Rate R μ_R, Recovery rate μ	0.1
Infection rate α	0.2

Table 4.1: Epidemic parameters used in simulations.

The color mapping is the following: *Sucseptible:* blue, *Exposed:* orange, *Infected:* red and *Recovered:* green.

4.2.2 SIS Model

Snapshots of the SIS model evolution on the network are shown in Figure 4.1. The simulation results and ODE solution are compared in Figure 1.1 (already shown in the main section of the review).

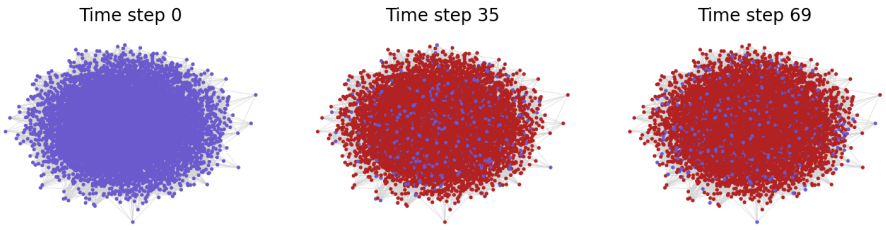

Figure 4.1: Snapshots at $t = 0$, $t = T/2$, and $t = T$ for the SIS model.

Mean-Field Equations

Letting $s = S/N$ and $i = I/N$ denote the fractions of susceptible and infected individuals in a population of size N, the corresponding mean-field equations for the fractions $s(t)$ and $i(t)$ are:

$$\frac{ds}{dt} = -\beta\langle k\rangle si + \mu_S i$$
$$\frac{di}{dt} = \beta\langle k\rangle si - \mu_S i$$

We define a binary state variable $\sigma_i(t)$ for each node and the infection probability $\rho(i,t) = \text{Prob}[\sigma_i(t) = 1]$. Assuming spatial homogeneity $\rho(i,t) = \rho(t)$ and statistical independence:

$$\text{Prob}[\sigma_i = 0, \sigma_j = 1] \approx (1-\rho)\rho. \tag{4.3}$$

The corresponding mean-field equation for the infection probability becomes:

$$\frac{d\rho}{dt} = -\mu\rho + \beta\sum_j A_{ij}(1-\rho)\rho. \tag{4.4}$$

In homogeneous networks, where each node has the same average degree $\langle k\rangle$, we approximate $\sum_j A_{ij} \approx \langle k\rangle$, yielding:

$$\frac{d\rho}{dt} = -\mu\rho + \beta\langle k\rangle(1-\rho)\rho. \tag{4.5}$$

This is a logistic-type equation that admits a steady-state solution. If $\beta > \mu/\langle k \rangle$, the infection persists in an endemic state.

The analytical solution of Eq. (4.5), assuming an initial condition $\rho(0) = \rho_0$, is:

$$\rho(t) = \rho_0 \frac{(\beta\langle k \rangle - \mu)e^{(\beta\langle k \rangle - \mu)t}}{\beta\langle k \rangle - \mu + \beta\langle k \rangle \rho_0 e^{(\beta\langle k \rangle - \mu)t}}. \tag{4.6}$$

This solution describes initial exponential growth followed by saturation at a steady-state value $\rho_\infty = 1 - \frac{\mu}{\beta\langle k \rangle}$.

In the early phase of the outbreak, when $\rho \ll 1$, we can approximate:

$$\rho(t) \approx \rho_0 e^{(\beta\langle k \rangle - \mu)t}. \tag{4.7}$$

At steady state, setting $d\rho/dt = 0$ in Eq. (4.5) leads to the threshold condition for sustained transmission:

$$\beta > \frac{\mu}{\langle k \rangle}.$$

This defines the basic reproduction number $R_0 = \beta\langle k \rangle/\mu$. The epidemic becomes endemic only if $R_0 > 1$. In our network, this gives a threshold value $\beta_c = 0.005$.

4.2.3 SI Model

The simulation results and ODE solution are compared in Figure 4.2.

Mean-Field Equation

The mean-field dynamics are governed by the following system of ordinary differential equations:

$$\frac{ds}{dt} = -\beta\langle k \rangle si$$
$$\frac{di}{dt} = \beta\langle k \rangle si$$

With $\langle k \rangle$ average degree of the network.

In the SI model, there is no recovery, so the probability of being infected can only increase:

$$\frac{d\rho}{dt} = \beta\langle k \rangle(1 - \rho)\rho. \tag{4.8}$$

The analytical solution of the mean-field equation (4.8), assuming an initial condition $\rho(0) = \rho_0$, is:

$$\rho(t) = \frac{\rho_0 e^{\beta\langle k \rangle t}}{1 - \rho_0 + \rho_0 e^{\beta\langle k \rangle t}}. \tag{4.9}$$

This is a logistic function describing initial exponential growth with rate $\beta\langle k \rangle$, eventually saturating at $\rho = 1$, corresponding to full infection of the population.

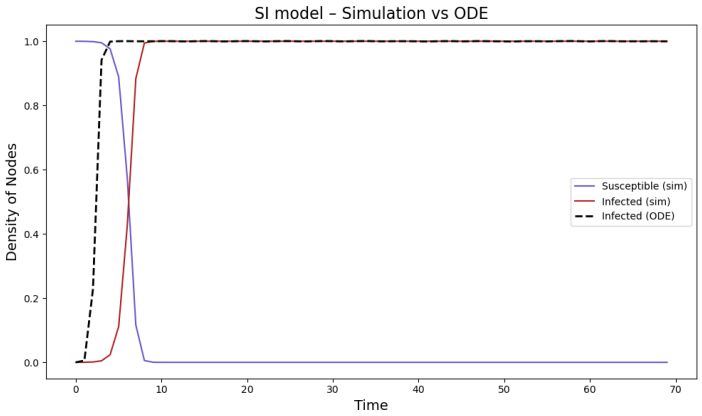

Figure 4.2: Simulation vs ODE integration for the SI model.

4.2.4 SIR Model

The simulation results and ODE solution are compared in Figure 4.3.

Mean-Field Equations

The corresponding mean-field equations for the fractions $s(t)$, $i(t)$ and $r(t)$ are:

$$\frac{ds}{dt} = -\beta\langle k\rangle si$$

$$\frac{di}{dt} = \beta\langle k\rangle si - \mu_R i$$

$$\frac{dr}{dt} = \mu_R i$$

The SIR model exhibits a stochastic regime in which the infection may die out due to random fluctuations, especially in the early stages.

Although the full model does not admit a closed-form analytical solution, qualitative insights can still be obtained by analyzing its asymptotic behavior as $t = \infty$. At $t = \infty$, we have that $i(\infty) = 0$ and thus $s(\infty) = 1 - r(\infty)$, hence the final state is fully characterized by the susceptible and recovered fractions.

$$1 - r(\infty) - s_0 e^{-r(\infty)\frac{\beta}{\mu_R}} = 0$$

This is a trascendental equation that cannot be solved analytically but it gives important hints on the behavior of the disease

- $\dfrac{\beta\langle k\rangle}{\mu_R} = R_0$, determines whether the disease can grow and spread.
- s_0 plays a central role in shaping the outbreak's outcome. If this fraction is sufficiently low, the infection cannot propagate effectively.

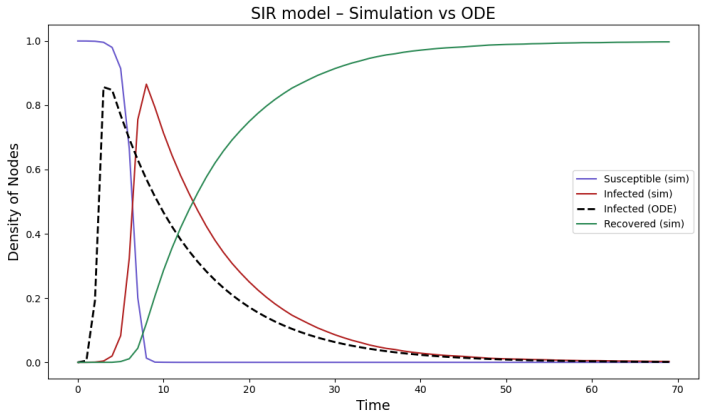

Figure 4.3: Simulation vs ODE integration for the SIR model.

4.2.5 SEIR Model

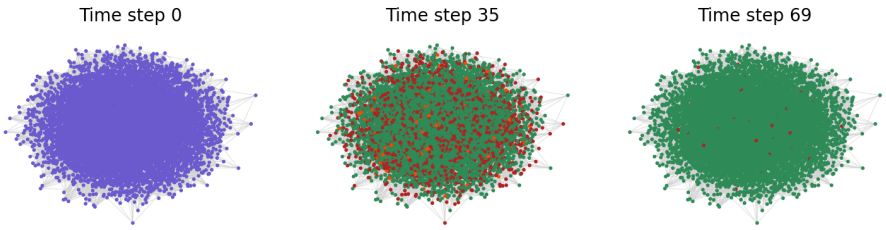

Figure 4.4: Snapshots at $t = 0$, $t = T/2$, and $t = T$ for the SEIR model.

Mean-Field Equations

The corresponding mean-field equations for the fractions $s(t)$, $i(t)$, $e(t)$ and $r(t)$ are:

$$\frac{ds}{dt} = -\beta\langle k\rangle si$$

$$\frac{de}{dt} = \beta\langle k\rangle si - \alpha e$$

$$\frac{di}{dt} = \alpha e - \mu i$$

$$\frac{dr}{dt} = \mu i$$

For very short latent periods—corresponding to the limit $\alpha \to \infty$, where α is the rate of progression from exposed to infectious—the SEIR model reduces to the classical SIR model, recovering its endemic behavior.

While the steady-state properties—such as the basic reproduction number R_0 and the final epidemic size—are often similar between SEIR and SIR models, the inclusion of an exposed compartment introduces a delay in the dynamics. This delay leads to

a noticeably slower initial growth of the infection, approximately proportional to the square root of time, compared to the exponential growth seen in the SIR model:

$$\rho_{\mathrm{SEIR}}(t) \approx \rho_0 e^{\left(\sqrt{4(R_0-1)\alpha\mu+(\alpha+\mu)^2}-(\alpha+\mu)\right)t/2} \approx \rho_0 e^{(\sqrt{R_0}-1)\mu t}, \tag{4.10}$$

$$\rho_{\mathrm{SIR}}(t) \approx \rho_0 e^{(R_0-1)\mu t}. \tag{4.11}$$

Although this difference vanishes at equilibrium, it has substantial implications during the early stages of an outbreak. Accurately capturing such temporal dynamics is crucial for effective early interventions and informed public health decisions.

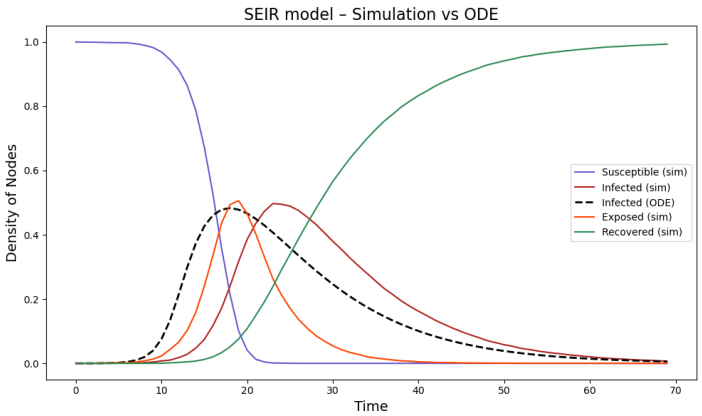

Figure 4.5: Simulation vs ODE integration for the SEIR model.

4.3 | Heterogeneous Mean Field Approximation

4.3.1 Finite size effects on the SIS critical threshold

Real-world networks are inherently finite, making it essential to account for finite-size corrections when evaluating epidemic thresholds. A common approach is to introduce an exponential cutoff in the degree distribution:

$$P(k) \simeq k^{-\gamma} e^{-\frac{k}{k_c}}$$

where k_c is a characteristic cutoff degree. For large k_c and degree exponent $2 < \gamma < 3$ the critical infection rate acquires a finite-size correction and is approximated by:

$$\beta_c \simeq \left(\frac{\mu k_c}{k_{min}}\right)^{\gamma-3}$$

4.3.2 SIR

In this appendix, I perform the heterogeneous mean-field analysis for the SIR model, following the methodology presented in the main text. We define the densities of

susceptible, infected, and recovered nodes of degree k at time t as $\rho_k^S(t)$, $\rho_k^I(t)$, and $\rho_k^R(t)$, respectively, with the final recovered density given by

$$\rho_\infty^R = \lim_{t\to\infty} \sum_k P(k)\rho_k^R(t).$$

The evolution equations for the infected and recovered densities read

$$\frac{d\rho_k^I(t)}{dt} = -\mu\rho_k^I(t) + \beta k \rho_k^S(t)\Gamma_k(t),$$

$$\frac{d\rho_k^R(t)}{dt} = \mu\rho_k^I(t),$$

where the susceptible density satisfies $\rho_k^S(t) = 1 - \rho_k^I(t) - \rho_k^R(t)$.

Here,

$$\Gamma_k(t) = \sum_{k'} \frac{k'-1}{k'} P(k'|k)\rho_{k'}^I(t),$$

represents the probability that a neighbor of a node with degree k is infected.

This formalism modifies the epidemic threshold, which becomes

$$\beta_c = \frac{\mu\langle k\rangle}{\langle k^2\rangle - \langle k\rangle}.$$

Importantly, for finite networks, the thresholds for the SIS and SIR models differ, i.e.,

$$\beta_c^{\text{SIS}} \neq \beta_c^{\text{SIR}}.$$

4.3.3 SI

In the absence of recovery, the SI model admits a degree-based mean-field description with:

$$\frac{d\rho_k(t)}{dt} = \beta k \left[1 - \rho_k(t)\right]\Theta(t), \qquad \Theta(t) = \sum_{k'} \frac{k'P(k')}{\langle k\rangle}\rho_{k'}(t).$$

Since no recovery occurs, the infection always spreads throughout the network and there is no epidemic threshold ($\beta_c = 0$).

4.3.4 SEIR

The SEIR model incorporates an exposed compartment with a finite rate of progression to infection. The degree-based equations read:

$$\begin{aligned}
\frac{d\rho_k^S}{dt} &= -\beta k \rho_k^S(t)\Theta(t),\\
\frac{d\rho_k^E}{dt} &= \beta k \rho_k^S(t)\Theta(t) - \alpha\rho_k^E(t),\\
\frac{d\rho_k^I}{dt} &= \alpha\rho_k^E(t) - \mu\rho_k^I(t),\\
\frac{d\rho_k^R}{dt} &= \mu\rho_k^I(t),
\end{aligned} \qquad \Theta(t) = \sum_{k'} \frac{k'P(k')}{\langle k\rangle}\rho_{k'}^I(t).$$

To compute the epidemic threshold, we linearize the system near the disease-free state. Assuming $\rho_k^E, \rho_k^I \ll 1$ and $\rho_k^S \approx 1$, the growth of ρ_k^I becomes:

$$\frac{d\rho_k^I}{dt} \approx \alpha\rho_k^E - \mu\rho_k^I, \quad \frac{d\rho_k^E}{dt} \approx \beta k\Theta - \alpha\rho_k^E.$$

Solving this linear system yields exponential growth when:

$$\frac{\beta\alpha\langle k^2\rangle}{\mu(\alpha+\mu)\langle k\rangle} > 1,$$

leading to the epidemic threshold:

$$\beta_c = \frac{\mu(\alpha+\mu)\langle k\rangle}{\alpha\langle k^2\rangle}.$$

As in the SIR and SIS cases, $\beta_c \to 0$ for scale-free networks with $2 < \gamma < 3$ in the limit $N \to \infty$, indicating the absence of a threshold in the thermodynamic limit.

4.3.5 Threshold Evaluation

Network structure

The simulations were performed on a Barabási–Albert (BA) network, a well-known model for generating scale-free networks characterized by a power-law degree distribution. The network was constructed with $N = 10^4$ nodes, where each new node is connected to $m = 4$ existing nodes during the network growth process. This generates a heterogeneous topology with a heavy-tailed degree distribution, which strongly influences epidemic dynamics and lowers the epidemic threshold compared to homogeneous networks.

The BA model captures the presence of highly connected hubs, which can significantly accelerate the spread of infections and contribute to the vanishing of the epidemic threshold in the thermodynamic limit.

SIS

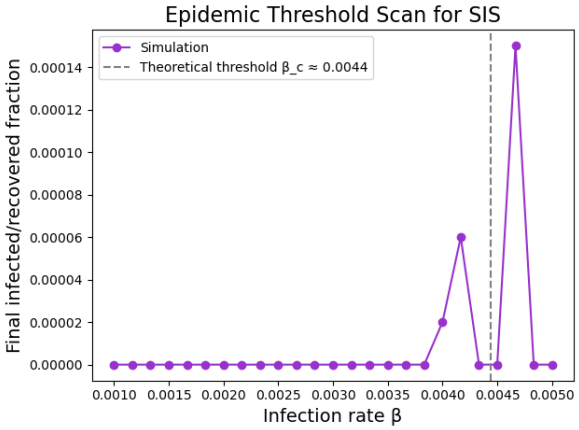

Figure 4.6: Epidemic threshold estimation for the SIS model on a heterogeneous network. Each point represents the average infected fraction over multiple runs at fixed infection rate β.

The theoretical epidemic threshold in the heterogeneous mean-field approximation is given by:

$$\beta_c = \frac{\mu\langle k\rangle}{\langle k^2\rangle}, \tag{4.12}$$

For the network under study, this gives $\beta_c \approx 0.0044$. However, in simulations, the estimated threshold appears slightly smaller. This discrepancy is due to stochastic effects, finite-size fluctuations , and the fact that the true threshold is better captured by the quenched mean-field theory:

$$\beta_c^{\mathrm{QMF}} = \frac{\mu}{\Lambda_{\max}}, \tag{4.13}$$

where $\Lambda_{\max}$ is the largest eigenvalue of the adjacency matrix. In scale-free networks, $\Lambda_{\max}$ can be larger than the mean-field estimate suggests, slightly lowering the empirical critical point observed in simulations.

SIR

In this case, I simulate the SIR model on the same Barabási–Albert network described previously. The theoretical epidemic threshold in the heterogeneous mean-field approx-

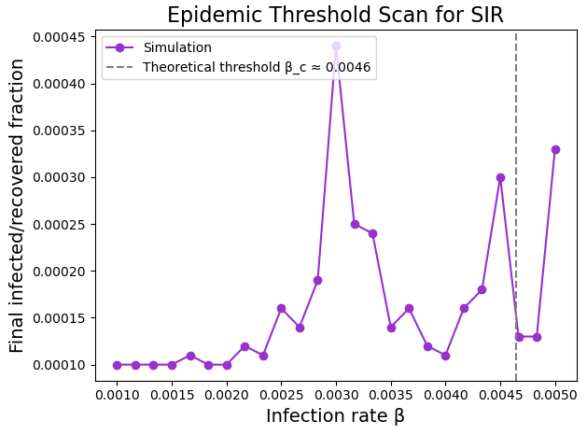

Figure 4.7: Epidemic threshold estimation for the SIS model on a heterogeneous network. Each point represents the average infected fraction over multiple runs at fixed infection rate β.

imation is given by:

$$\beta_c = \frac{\mu\langle k\rangle}{\langle k^2\rangle - \langle k\rangle}$$

For the network under study, this gives $\beta_c \approx 0.0046$. This threshold indicates the critical point above which a macroscopic fraction of the population becomes infected and then recovers. Once again, we see the discrepancy from the theoretical threshold.

4.4 | Epidemic spreading on patchy metapopulations: SI, SIS, SIR, SEIR in homogeneous mean-field approximation

Invasion Threshold in the SI Model

The SI model assumes that once infected, individuals remain infectious forever. As a result, there is no recovery and thus no local epidemic threshold; local outbreaks always grow once seeded. The only condition for the epidemic to invade the metapopulation is that infected individuals successfully travel and seed neighboring patches.

In this case, the global invasion depends solely on mobility and the network structure, as there is no saturation or recovery. Every infected individual has infinite infectious duration, so the cumulative probability of infecting neighboring patches approaches one. The focus is therefore on ensuring that the infection reaches a critical number of patches for widespread invasion.

Invasion Threshold in the SIS Model

In the SIS model, individuals can recover and return to the susceptible state. An infected individual remains infectious for an average time μ^{-1}, and if $R_0 > 1$, the infection reaches an endemic steady state within each patch.

As with the SIR model, a global invasion threshold can be defined using a tree-like approximation. However, the quantity α is no longer the final size of the outbreak but rather the stationary fraction of infected individuals within a patch.

The global reproductive number for SIS is given by:

$$R^* = p\bar{N}\alpha\mu^{-1}\frac{\bar{k}-1}{\bar{k}}(R_0 - 1),$$

and global invasion occurs when $R^* > 1$.

Invasion Threshold in the SEIR Model

The SEIR model introduces a latent (exposed) compartment E, capturing the delay between infection and the onset of infectiousness. The disease progression is $S \to E \to I \to R$, where exposed individuals become infectious at rate ϵ, and infectious individuals recover at rate μ. The change of notation from α to ϵ for the infection rate is needed because in this notation α is used as the rate of individuals that become infectious during the outbreak.

This latency reduces the effective transmissibility and thus raises the critical threshold. The theoretical threshold in the homogeneous mean-field approximation becomes:

$$\beta_c = \mu(\mu + \epsilon)\frac{\langle k\rangle}{\epsilon\langle k^2\rangle}.$$

Global invasion in the metapopulation is still governed by a condition of the form $R^* > 1$, but now the term α accounts for both delayed infectiousness and the final size of the outbreak, typically lower than in SIR.

4.5 | Use of ChatGPT

In this project, ChatGPT [12] primarily assisted in the final revision of the review, refining my initial draft to enhance clarity, professionalism, and appropriateness of language. It also helped in the coding part, suggesting the best structure to tackle the epidemic simulations, and in finding the papers related to the homogeneous and heterogeneous mean field approximations.

4.6 | Further acknowledgments

For the sake of correctness, I acknowledge that part of the material and derivations presented in this review are based on the lecture slides from the course on epidemic modeling taught by Prof. Sandro Meloni.

5 | Bibliography

[1] William Ogilvy Kermack and Anderson Gray McKendrick. A contribution to the mathematical theory of epidemics. *Proceedings of the Royal Society of London. Series A, Containing Papers of a Mathematical and Physical Character*, 115(772):700–721, 1927.

[2] Neil M Ferguson, Daniel Laydon, Gemma Nedjati-Gilani, et al. Impact of non-pharmaceutical interventions (npis) to reduce covid-19 mortality and healthcare demand. https://doi.org/10.25561/77482, 2020. Imperial College London Report 9, [Accessed 8-Jul-2025].

[3] Seth Flaxman, Swapnil Mishra, Axel Gandy, et al. Estimating the effects of non-pharmaceutical interventions on covid-19 in europe. *Nature*, 584(7820):257–261, 2020.

[4] Giulia Giordano, Franco Blanchini, Raffaele Bruno, et al. Modelling the covid-19 epidemic and implementation of population-wide interventions in italy. *Nature Medicine*, 26(6):855–860, 2020.

[5] Romualdo Pastor-Satorras and Alessandro Vespignani. Epidemic spreading in scale-free networks. *Physical Review Letters*, 86(14):3200–3203, 2001.

[6] Vittoria Colizza, Romualdo Pastor-Satorras, and Alessandro Vespignani. Invasion threshold in heterogeneous metapopulation networks. *Nature Physics*, 3(4):276–282, 2007.

[7] Vittoria Colizza and Alessandro Vespignani. Epidemic processes in complex networks. *Journal of Theoretical Biology*, 251(3):450–467, 2008.

[8] Frank Ball, Denis Mollison, and Gianpaolo Scalia-Tomba. Epidemics with two levels of mixing. *The Annals of Applied Probability*, 7(1):46–89, 1997.

[9] Paul C Cross, James O Lloyd-Smith, and Wayne M Getz. Dual hierarchies in metapopulation disease dynamics. *Ecology Letters*, 10(6):587–595, 2007.

[10] James D Murray. *Mathematical Biology: I. An Introduction*, volume 17 of *Interdisciplinary Applied Mathematics*. Springer, third edition, 2005.

[11] Vittoria Colizza and Alessandro Vespignani. Epidemic modeling in metapopulation systems with heterogeneous coupling pattern: Theory and simulations. *Journal of Theoretical Biology*, 251(3):450–467, 2008.

[12] OpenAI. Chatgpt (feb 15, 2025 version), 2025. Accessed: 2025-02-15.